Biochemical and Biophysical Research Communications 497 (2018) 467–472

Contents lists available at ScienceDirect

Biochemical and Biophysical Research Communications

journal homepage: www.elsevier.com/locate/ybbrc

GhoT of the GhoT/GhoS toxin/antitoxin system damages lipid membranes by forming transient pores

Jun-Seob Kim, Allen B. Schantz, Sooyeon Song, Manish Kumar, Thomas K. Wood*

Department of Chemical Engineering, Pennsylvania State University, University Park, PA, 16802-4400, USA

ARTICLE INFO

Article history:
Received 4 January 2018
Accepted 10 January 2018
Available online 19 February 2018

Keywords:
GhoT
Toxin
Membranes

ABSTRACT

GhoT is a bacterial toxin of the type V toxin/antitoxin system that allows *Escherichia coli* to reduce its metabolism in response to oxidative and bile stress. GhoT functions by increasing membrane permeability and reducing both ATP levels and the proton motive force. However, how GhoT damages the inner membrane has not been elucidated. Here we investigated how GhoT damages membranes by studying its interaction with lipid bilayers and determined that GhoT does not cause macroscopic disruption of the lipid bilayer to increase membrane permeability to the dye carboxyfluorescein. Using circular dichroism, we found that GhoT forms an alpha helical structure in lipid bilayers that agrees with the structure predicted by the I-TASSER protein structure prediction program. The structure generated using I-TASSER was used to conduct coarse-grained molecular dynamics simulations, which indicate that GhoT damages the cell membrane, as a multimer, by forming transient transmembrane pores.

1. Introduction

Toxin/antitoxin (TA) systems in bacteria reduce the metabolism of cells to allow them to weather nutritional, oxidative, and antibiotic stress [1]. TA systems consist of two major parts, a toxin protein that disrupts essential cellular processes and an antitoxin (protein or RNA) that inhibits the activity of the toxin [2]. Without stress, toxins are inactivated, but during stress, antitoxins are degraded and the toxin reduces metabolism [2].

TA systems are classified into seven different types based on how the antitoxin neutralizes the toxin. In type I systems (e.g., Hok/Sok), the antitoxin RNA interferes with the translation of the toxin [3]. In type II systems (e.g., CcdB/CcdA), the antitoxin protein binds to toxin and inhibits its activity [4]. In type III systems (e.g., ToxN/ToxI), the antitoxin RNA binds the toxin to inhibit it [5]. In type IV systems (e.g., CbtA/CbeA), the antitoxin protein inhibits the toxin by binding its target [6]. In type V systems (e.g., GhoT/GhoS), the antitoxin is a specific RNase that cleaves the toxin's mRNA [7]. In type VI systems (e.g., SocB/SocA), the antitoxin protein promotes the degradation of the toxin [8]. In type VII systems (e.g., Hha/TomB), the antitoxin is an enzyme that oxidizes specifically the toxin to inactivate it [9].

The cellular targets of toxin proteins of TA systems vary and include (i) replication by inhibiting DNA gyrase (CcdB, ParE) [10,11], (ii) translation by cleaving many mRNA (SymE, MazF, HicA, RelE, MqsR) [7,10–13], (iii) translation by phosphorylating EF-Tu (HipA) [14], (iv) cellular structure by inhibiting FtsZ (YeeV, CptA) [6,15] and (v) adenosine triphosphate (ATP) synthesis by cell membrane damage (Hok, TisB) [16,17].

Previously, we found the first type V TA system, GhoT/GhoS, in which ribonuclease GhoS (antitoxin) cleaves the mRNA of GhoT toxin to inhibit its translation [18]. The GhoT/GhoS TA system is also controlled by the MqsR-MqsA TA system (type II) in which toxin MqsR degrades specifically the GhoS antitoxin mRNA during oxidative stress and bile stress (the GhoT mRNA lacks MqsR cleavage sites) [19,20]. Critically, the formation of persister cells by MqsR depends partially on toxin GhoT [18]. Production of toxin GhoT damages the cell membrane and reduces ATP levels, the proton motive force (PMF), and cell growth [12]. GhoT consists of 57 amino acids, 68% of which are hydrophobic. GhoT is predicted to contain an amphiphilic a-helix, and localization of the non-toxic GhoT variant (GhoT F38R) indicates GhoT is membrane protein [12].

In this study, the mechanism of GhoT toxicity was determined using lipid bilayers to mimic the *E. coli* inner membrane [21]. Circular dichroism (CD) showed that GhoT changes its conformation in the presence of lipids to form a structure that agrees with protein modeling results [12]; hence, we confirm that GhoT is a membrane protein with alpha-helical structure. Furthermore, GhoT does not

* Corresponding author.
E-mail address: twood@engr.psu.edu (T.K. Wood).

https://doi.org/10.1016/j.bbrc.2018.01.067
0006-291X/

cause macroscopic disruption of liposomes. Simulations of GhoT in the lipid bilayer indicate that GhoT damages the cell membrane by forming transient pores through the membrane. This mechanism is different from that of many toxins, such as TisB of the TisB/IstR TA system [22], that disrupt the membrane by forming permanent pores. However, other peptides (especially antimicrobial peptides) cause leakage by transiently forming pore-like aggregates that disrupt the sharp hydrophobic/hydrophilic interface within the cell membrane [23,24], similarly to what we observe with GhoT.

2. Materials and methods

2.1. Bacterial strains and culture conditions

E. coli BW25113 Δ*ghoS* with plasmids pCA24N [25], pCA24N-GhoT [25], and pCA24N-GhoT F38R [12] were utilized; chloramphenicol (34 μg/mL) was used to retain the plasmids. To induce protein expression, isopropyl β-*D*-1-thiogalactopyranoside (0.1 mM) was added after 1 h. Strains were grown in LB medium [26] at 37 °C with shaking at 250 rpm. To test for membrane damage, GhoT and GhoT F38R (0.25 μg/mL) were electroporated into BW25113 (200 Ω, 1.25 kV) [26].

2.2. Peptide synthesis

GhoT and GhoT F38R peptides were synthesized by Lifetein LLC (New Jersey, USA). The purities the syntheses were over 90% as confirmed by HPLC, and the identities of the proteins were confirmed by mass spectrum (MS). The peptides were dissolved in DMSO or methanol as indicated.

2.3. Determination of secondary structures of GhoT via CD spectrum

Egg L-α-phosphatidylcholine (PC, Avanti, #840051) and brain L-α-phosphatidylserine (PS, Avanti, #840032) lipids were dissolved in chloroform (10 mg/mL), and GhoT was dissolved in methanol (1 mg/mL). To make 1 mL of liposomes (1 mg/mL), 179 μL of egg PC and 21 μL of brain PS were mixed (1:1) with 100 μL of GhoT in a round tube at a final molar ratio of peptide:lipid = 1:85. The chloroform and methanol were removed by a rotary evaporator (180 rpm, 420 mbar) at 42 °C. Lipid and peptide films were incubated in the vacuum chamber for an additional 3 h to ensure evaporation of chloroform and methanol. 1 mL of 100 mM sodium phosphate buffer (pH 7.4) was added to the lipid-peptide films and incubated overnight at 4 °C to dissolve the films in buffer via a stirrer. The mixture of lipid and peptides dissolved in phosphate buffer was extruded through track-etched polycarbonate membrane filters (Whatman, Maidstone, UK) with diameters through 400 nm (5 times), 200 nm (5 times), 100 nm (10 times) to prepare the liposomes containing GhoT at a size of ~100 nm diameter. The quality of the liposomes was determined by dynamic light scattering (Zetasizer Nano ZS, Malvern). The CD spectrum was analyzed by Jasco J-1500 CD Spectrometer (Easton, MD, USA).

2.4. Liposomal content release assay

Egg PC (Avanti, 840051) and brain PS (Avanti, 840032) stocks were dissolved in chloroform (10 mg/mL) and used to prepare the PC-PS liposomes. *E. coli* total lipid extracts (Avanti, 100500) were dissolved in chloroform (10 mg/mL) and used for the *E. coli* liposomes. A 50 mM 5(6)-carboxyfluorescein (CF) (Sigma-Aldrich, 21877) solution was prepared in 50 mM HEPES buffer (pH 7.4). CF solution (2 mL, 50 mM) was added to the lipid film and incubated overnight at 4 °C to dissolve the lipid film in solution by stirring. The lipid dissolved in 50 mM carboxyfluorescein solution was extruded through a 100 nm polycarbonate filter (Whatman, Maidstone, UK) 10 times to generate a consistent 100 nm diameter liposomes. The size of all the prepared liposomes were confirmed by dynamic light scattering (Zetasizer Nano ZS, Malvern). Liposomes (50 μL) were mixed with 40 μL of 50 mM HEPES buffer to make a final concentration of 0.5 mg/mL and pre-incubated in the fluorometer (TECAN, Infinite M200 pro) for 10 min. Various concentrations of native GhoT and GhoT F38R (final conc. 0.25, 0.125, 0.05 mg/mL) dissolved in DMSO were added to the liposomes. The fluorescence signal was measured with excitation at 490 nm and emission at 520 nm (gain 42) at 25 °C. Triton X-100 (1%) was added to determine the value for 100% release of carboxyfluorescein. The percentage of CF release was calculated as $\frac{(CF_t - CF_0)}{(CF_{tx-100} - CF_0)} \times 100$.

2.5. Simulations

From the known amino acid sequences of the native and F38R variant GhoT peptides, we used the I-TASSER structure prediction program [27,28] to determine the most probable structure for each peptide. We then converted the all-atom structures obtained from I-TASSER to MARTINI coarse-grained structures [29–32] using the martinize.py script [30,31]. We then combined these structures with lipids, either anionic 1,2-dipalmitoyl-sn-glycero-3-phosphoglycerol (DPPG) or zwitterionic 1,2-dipalmitoyl-sn-glycero-3-phosphocholine (DPPC), and water, also represented using the MARTINI coarse-grained model. Initial configuration construction and simulations were both conducted using the Gromacs program for biological simulations [33]. Images of our simulations were made using Visual Molecular Dynamics software [34]. For the remaining simulation details, please see the supplementary methods.

3. Results

3.1. Conformational changes of GhoT in a lipid bilayer

Since GhoT is very toxic, it has never been visualized by SDS-PAGE or Western blotting [12]; hence, in order to study it, we synthesized GhoT chemically. GhoT is poorly soluble so it was dissolved in methanol.

The secondary structure of GhoT in the presence or absence of a lipid bilayer was determined based on its CD spectrum. The *E. coli* inner membrane is a highly impermeable bilayer. Since the *E. coli* inner membrane consists of up to 25% of negatively charged lipids (phosphatidylglycerol (PG) and cardiolipin) [35], we used PC-PS liposomes (9:1 ratio) which contains 10% of negatively charged lipids (PS). As expected as a membrane protein, GhoT displayed a conformational secondary structure in the presence of the lipid bilayer while no secondary structure was determined in the absence of lipid (Fig. 1). The CD spectrum had a negative peak around 222 nm and 208 nm and a positive peak around 195 nm. This result confirms that GhoT forms an α-helix when it is contacted with lipids as previously predicted [12].

3.2. GhoT promotes release of liposomal contents

In the previous research, membrane damage, depletion of intracellular ATP, and disruption of the proton motive force by GhoT was demonstrated *in vivo* [12]. To show directly that GhoT damages membranes, a liposomal contents release assay was performed. CF is a self-quenching fluorescein that fluoresces only at low concentrations [36]; hence, damage of membranes is monitored by the % CF released from liposomes. Since fluorescence generated by CF started to increase at 25 mM (Fig. S1), small unilamellar liposomes

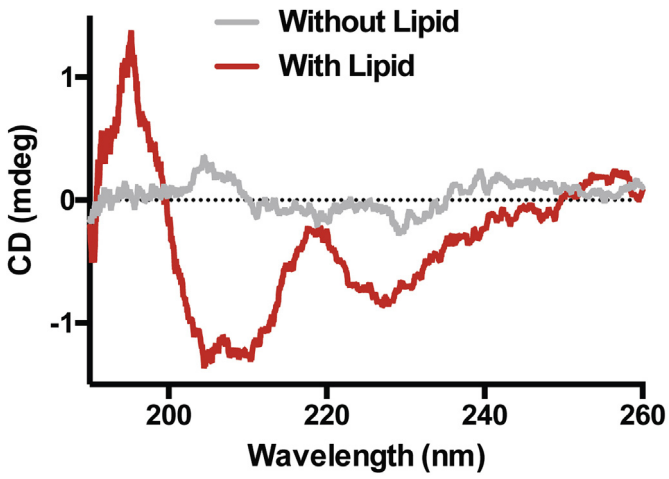

Fig. 1. Secondary structure of GhoT in a PC-PS lipid bilayer determined by CD. GhoT was analyzed by circular dichroism to determine its secondary structure in presence or absence of PC-PS lipid. GhoT displays α-helical structure only with lipid.

containing 50 mM CF were employed to determine the effect of GhoT. We found GhoT damaged the liposomes to cause 27% of the CF to be released in 10 min in PC-PS liposomes at 0.25 mg/mL (a molar ratio of peptide:lipid ≈ 1:17) (Fig. 2). The CF released was determined with various GhoT concentrations, and the percentages of CF release were proportional to GhoT concentration (Fig. 2). This provides evidence that GhoT damages the membrane by being incorporated into the lipid bilayer.

Since the GhoT F38R variant does not show any lytic activity *in vivo* [12], the CF contents release assay with GhoT F38R was performed. Unexpectedly, GhoT F38R showed similar CF release with native GhoT (about 30%) (Fig. 3A), which is in contrast to the *in vivo* results where production of GhoT F38R had no effect on cell viability. We confirmed these results and found GhoT F38R does not inhibit growth while GhoT ceases cell growth (Fig. 3B).

To investigate these results further, we tried adding GhoT from the outside of the cells by electroporating GhoT and GhoT F38R into BW25113. After 1 h, both GhoT and GhoT F38R caused similar cell settling (data not shown). This indicates that GhoT F38R can damage the cell membrane if it is added externally.

Although the PC-PS liposomes from eucaryotes (egg and brain) that we used initially (Fig. 2A) contain negatively-charge lipids, natural *E. coli* lipids might show different results due to their different composition. To investigate whether GhoT disrupts *E. coli*-derived lipids, we performed the contents release assay with GhoT and GhoT F38R using a liposome made from an *E. coli* total lipid extract. Both GhoT and GhoT F38R released similar amounts of CF with the *E. coli* liposome, although the amount of CF released was 70% lower than that with PC-PS liposomes (e.g., 9% CF release with *E. coli* liposomes and 27% CF release with PC-PS liposome) (Fig. S2). This result indicates our PC-PS model for GhoT activity is suitable.

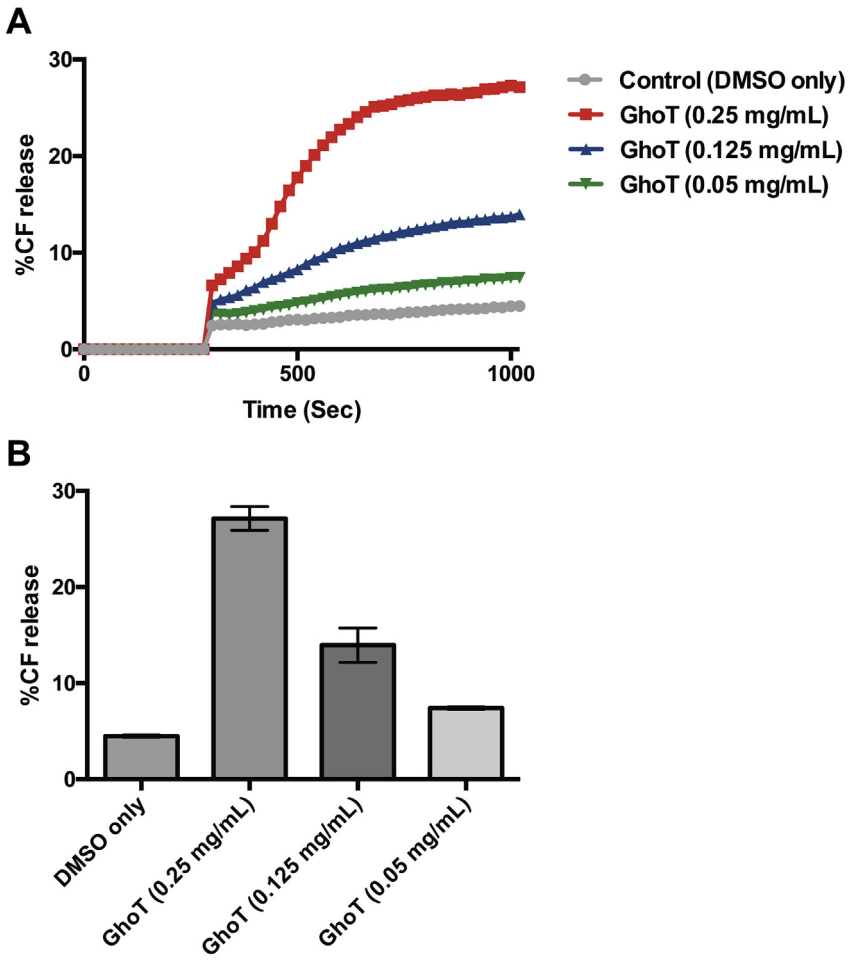

Fig. 2. Liposomal contents release assay by GhoT. (A) GhoT accelerates the release of CF from PC-PS liposomes based on its concentration. (B) CF released (%) by GhoT treatment.

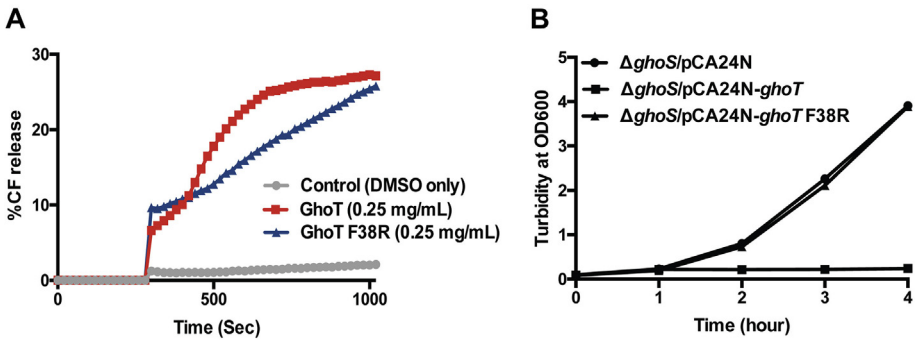

Fig. 3. Comparison GhoT and GhoT F38R activities. (A) Both GhoT and GhoT F38R show similar CF release with PC-PS liposomes. (B) *in vivo* production of GhoT F38R in *E. coli* from plasmid pCA24N did not show any toxicity.

3.3. GhoT does not induce the macroscopic disruption of lipid membrane

Since GhoT causes CF release from liposomes, the size distribution of PC-PS liposomes treated by GhoT was investigated to see whether GhoT triggers a macroscopic disruption of liposomes (Fig. S3). As a positive control, treatment of triton X-100 (1%) showed macroscopic disruption of liposomes via dynamic light scattering (DLS), and the size distribution of the remaining liposomes was shifted to the left (Figs. S3A and B), indicating smaller sizes of less than 10 nm. The treatment of DMSO (1%), as negative control, did not show any changes of size distribution as expected (Fig. S3C). GhoT (0.25 μg/mL) also did not show any changes of liposome size (100 nm) while there was undefined signal around 5000 nm which is a signal form peptide aggregation that could be observed with GhoT samples lacking liposomes (Fig. S3D). This result indicates that GhoT peptides does not induce the macroscopic disruption by itself, rather, they make small pore or leakage.

3.4. Membrane charge is important for GhoT activity

Since GhoT released less CF in *E. coli* liposomes compared to PC-PS liposomes (Fig. S2 vs. Fig. 2a), we tested for the release of CF from pure PC liposomes which contains only neutral lipid to investigate whether membrane charge can affect GhoT activity. Without negatively-charged lipids, GhoT had less effect in the contents release assay (Fig. S4). With PC-PS (9:1) liposomes, GhoT release about 30% of the CF but with pure PC liposomes, GhoT released only 12%. This result indicates that the membrane surface charge plays an important role for the activity of GhoT during its disruption of the lipid bilayer.

3.5. GhoT damages the lipid membrane by forming transient pores

Using our coarse-grained molecular dynamics simulations, we examined the interaction of GhoT with lipid bilayers. We attempted to address (i) whether GhoT forms structures that span the lipid bilayer and disrupts PMF, (ii) whether the structures are pores, (iii) how many peptides are required, and (iv) does the charge of the lipid bilayer matter. In addition, we tested whether disruption of the lipid bilayer such as by electroporation changes the membrane/peptide interactions.

In simulations in which a single GhoT peptide interacts with a lipid bilayer, we found that the GhoT peptide binds to the membrane surface but does not take on a transmembrane configuration. In contrast, when multiple native GhoT peptides are added to a lipid membrane (made from either anionic or zwitterionic lipids), peptides can insert into the membrane and form transmembrane aggregates. For simulations using an anionic lipid bilayer, a transmembrane trimer formed in one of five trials, whereas for simulations using a zwitterionic lipid bilayer, a transmembrane aggregate formed in three of five trials (a trimer, a pentamer, and a hexamer). The lack of a common shape suggests these aggregates can take the form of transient transmembrane pores that allow the passage of water through the membrane. Taken together, these results suggest that the native peptide can bind to a lipid membrane (either anionic or zwitterionic), and that membrane-bound GhoT oligomers (of at least trimer size in our simulations) can form transmembrane structures that allow leakage across the membrane, potentially disrupting the PMF and ATP synthesis.

In contrast, simulations that combine the GhoT F38R variant peptides with a lipid bilayer (anionic or zwitterionic), show only surface-bound aggregates and no transmembrane aggregate formation (5 simulations were run using zwitterionic lipids and 5 with anionic lipids). However, when a GhoT F38R peptide is combined with lipids when they are self-assembling in solution (i.e., mimicking the damaged membranes after electroporation), the GhoT F38R peptide can incorporate into the lipid bilayer as it forms. In the case where the peptides are introduced during self-assembly of lipids, the peptide has a transmembrane configuration in 3/5 simulations using anionic lipids and 4/5 simulations using zwitterionic lipids. In the remaining simulations, GhoT F38R binds to the lipid bilayer surface but doesn't span the membrane. This is similar to the simulation results for lipid bilayer self-assembly in the presence of native GhoT peptides: 3/4 simulations using anionic lipids and 2/4 simulations using zwitterionic lipids result in a membrane-spanning native peptide. Taken together with the protein insertion simulations discussed earlier, these membrane self-assembly simulations suggest that single peptides (both native GhoT and F38R variant) bind to the lipid bilayer surface and can insert into a lipid membrane as it forms. However, the F38R substitution appears to prevent the peptide from inserting into an existing lipid bilayer, and multiple peptides are required for transmembrane aggregate formation even for the native peptide. Interactions between the peptides and the lipid bilayer are shown in Fig. 4 and Fig. S6, and simulations mimicking electroporation are shown in Fig. S5. Movies for each simulation shown in these two figures are given as supplemental files.

4. Discussion

Each toxin protein in TA systems has an unique mechanism to reduce cell metabolism [2]. In this paper, we probed the mechanism of GhoT, the first type V toxin, by *in vitro* means. Using CD, we determined GhoT has an α-helical structure only in liposomes (Fig. 1). Using artificial liposomes, we determined that GhoT

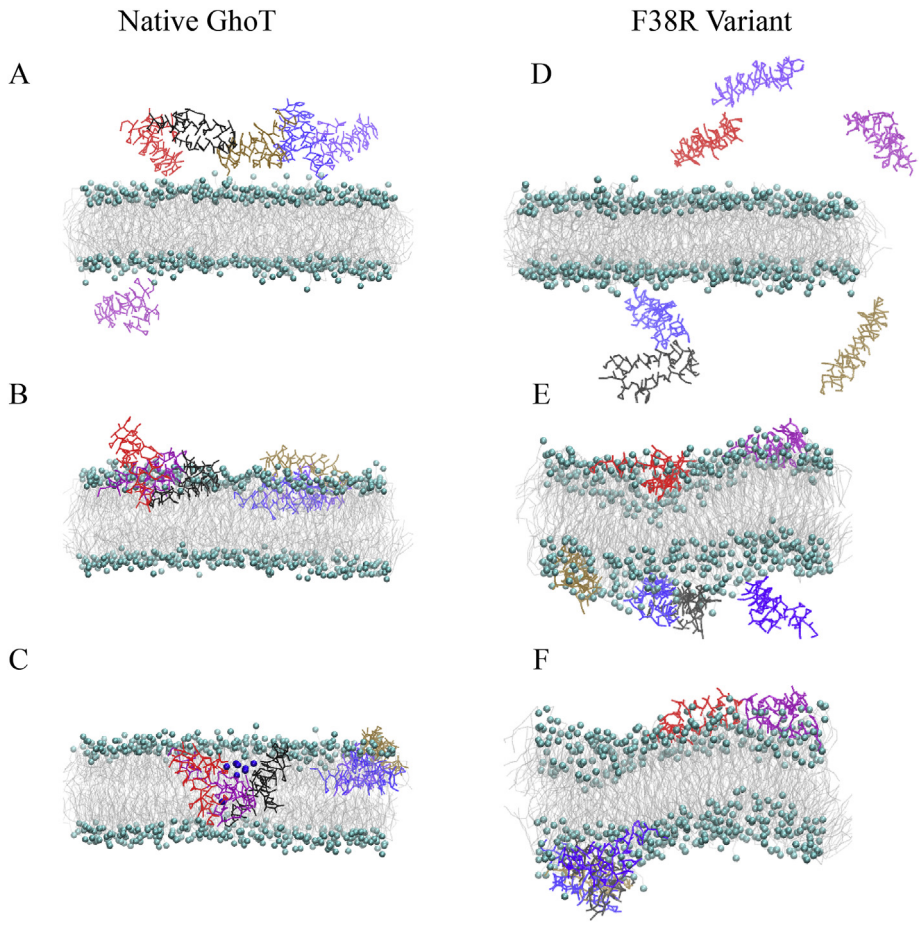

Fig. 4. Simulations showing that native GhoT forms multimeric transmembrane aggregates, while variant F38R remains surface-bound. Panels A-C show a simulation with 6 native GhoT peptides and 512 DPPC lipids at times 0 ns (A), 188 ns (B), and 500 ns (C). In this simulation, the peptides bind to the membrane surface and then form a trimeric transmembrane pore, which allows water to permeate across the membrane as shown in Panel C. Panels D-F show a simulation with 6 GhoT F38R variant peptides and 512 DPPG lipids at times 0 ns (D), 70 ns (E), and 1000 ns (F). The peptides quickly bind to the membrane surface and deform the membrane, but did not form a transmembrane structure.

damages the lipid membrane (Fig. 2) without massive disruption (Fig. S3), and molecular dynamics simulations suggest GhoT forms transient pores. Surprisingly, we found that the GhoT F38R variant, shown to be non-toxic *in vivo* (Fig. 3B), also damages the membrane (Fig. 3A). By adding GhoT F38R to the cell via electroporation, we found that GhoT F38R causes the cells to die in a manner similar to native GhoT. These results indicate GhoT F38R does not work in the cell even though it has a similar capacity to damage the cell membrane like GhoT. One possible explanation for the toxicity of GhoT F38R *in vitro* and after electroporation is that membrane disruption by electroporation and fluidization by DMSO may promote protein insertion. Coarse-grained simulations show that F38R peptides can insert into disrupted lipid bilayers, but did not show them to insert into intact lipid bilayers, suggesting that the F38R substitution may disrupt the peptide's ability to transition from a surface-bound to a transmembrane state after binding to an intact lipid membrane.

Conflicts of interest

The authors declare no competing financial interests.

Acknowledgments

This work was supported by the Army Research Office (W911NF-14-1-0279) and funds derived from the Biotechnology Endowed Professorship at the Pennsylvania State University.

Appendix A. Supplementary data

Supplementary data related to this article can be found at https://doi.org/10.1016/j.bbrc.2018.01.067.

Transparency document

Transparency document related to this article can be found online at https://doi.org/10.1016/j.bbrc.2018.01.067.

References

[1] X. Wang, T.K. Wood, Toxin-antitoxin systems influence biofilm and persister cell formation and the general stress response, Appl. Environ. Microbiol. 77 (2011) 5577–5583.
[2] R. Page, W. Peti, Toxin-antitoxin systems in bacterial growth arrest and persistence, Nat. Chem. Biol. 12 (2016) 208–214.
[3] K. Gerdes, F.W. Bech, S.T. Jorgensen, A. Lobner-Olesen, P.B. Rasmussen, T. Atlung, L. Boe, O. Karlstrom, S. Molin, K.v. Meyenburg, Mechanism of postsegregational killing by the *hok* gene product of the *parB* system of plasmid R1 and its homology with the RelF gene product of the *E. coli relB* operon, EMBO J. 5 (1986) 2023–2029.
[4] T. Ogura, S. Hiraga, Mini-F plasmid genes that couple host cell division to plasmid proliferation, Proc. Natl. Acad. Sci. U. S. A. 80 (1983) 4784–4788.
[5] P.C. Fineran, T.R. Blower, I.J. Foulds, D.P. Humphreys, K.S. Lilley, G.P.C. Salmond, The phage abortive infection system, ToxIN, functions as a protein–RNA toxin–antitoxin pair, Proc. Natl. Acad. Sci. U. S. A. 106 (2009) 894–899.

[6] H. Masuda, Q. Tan, N. Awano, K.-P. Wu, M. Inouye, YeeU enhances the bundling of cytoskeletal polymers of MreB and FtsZ, antagonizing the CbtA (YeeV) toxicity in *Escherichia coli*, Mol. Microbiol. 84 (2012) 979–989.
[7] X. Wang, D.M. Lord, H.Y. Cheng, D.O. Osbourne, S.H. Hong, V. Sanchez-Torres, C. Quiroga, K. Zheng, T. Herrmann, W. Peti, M.J. Benedik, R. Page, T.K. Wood, A new type V toxin-antitoxin system where mRNA for toxin GhoT is cleaved by antitoxin GhoS, Nat. Chem. Biol. 8 (2012) 855–861.
[8] Christopher D. Aakre, Tuyen N. Phung, D. Huang, Michael T. Laub, A bacterial toxin inhibits DNA replication elongation through a direct interaction with the β sliding clamp, Mol Cell 52 (2013) 617–628.
[9] O. Marimon, J.M.C. Teixeira, T.N. Cordeiro, V.W.C. Soo, T.L. Wood, M. Mayzel, I. Amata, J. García, A. Morera, M. Gay, M. Vilaseca, V.Y. Orekhov, T.K. Wood, M. Pons, An oxygen-sensitive toxin–antitoxin system, Nat. Commun. 7 (2016) 13634.
[10] T. Miki, J.A. Park, K. Nagao, N. Murayama, T. Horiuchi, Control of segregation of chromosomal DNA by sex factor F in *Escherichia coli*. Mutants of DNA gyrase subunit A suppress letD (ccdB) product growth inhibition, J. Mol. Biol. 225 (1992) 39–52.
[11] Y. Jiang, J. Pogliano, D.R. Helinski, I. Konieczny, ParE toxin encoded by the broad-host-range plasmid RK2 is an inhibitor of Escherichia coli gyrase, Mol. Microbiol. 44 (2002) 971–979.
[12] H.Y. Cheng, V.W. Soo, S. Islam, M.J. McAnulty, M.J. Benedik, T.K. Wood, Toxin GhoT of the GhoT/GhoS toxin/antitoxin system damages the cell membrane to reduce adenosine triphosphate and to reduce growth under stress, Environ. Microbiol. 16 (2014) 1741–1754.
[13] B.L. Brown, S. Grigoriu, Y. Kim, J.M. Arruda, A. Davenport, T.K. Wood, W. Peti, R. Page, Three dimensional structure of the MqsR: MqsA complex: a novel toxin:antitoxin pair comprised of a toxin homologous to RelE and an antitoxin with unique properties, PLoS Pathog. 5 (2009), e1000706.
[14] M.A. Schumacher, K.M. Piro, W. Xu, S. Hansen, K. Lewis, R.G. Brennan, Molecular mechanisms of HipA-mediated multidrug tolerance and its neutralization by HipB, Science 323 (2009) 396–401.
[15] H. Masuda, Q. Tan, N. Awano, Y. Yamaguchi, M. Inouye, A novel membrane-bound toxin for cell division, CptA (YgfX), inhibits polymerization of cytoskeleton proteins, FtsZ and MreB, in Escherichia coli, FEMS Microbiol. Lett. 328 (2012) 174–181.
[16] K. Gerdes, F.W. Bech, S.T. Jorgensen, A. Lobner-Olesen, P.B. Rasmussen, T. Atlung, L. Boe, O. Karlstrom, S. Molin, K. von Meyenburg, Mechanism of postsegregational killing by the hok gene product of the parB system of plasmid R1 and its homology with the relF gene product of the E. coli relB operon, EMBO J 5 (1986) 2023–2029.
[17] P.A. Gurnev, R. Ortenberg, T. Dorr, K. Lewis, S.M. Bezrukov, Persister-promoting bacterial toxin TisB produces anion-selective pores in planar lipid bilayers, FEBS Lett. 586 (2012) 2529–2534.
[18] X.X. Wang, D.M. Lord, H.Y. Cheng, D.O. Osbourne, S.H. Hong, V. Sanchez-Torres, C. Quiroga, K. Zheng, T. Herrmann, W. Peti, M.J. Benedik, R. Page, T.K. Wood, A new type V toxin-antitoxin system where mRNA for toxin GhoT is cleaved by antitoxin GhoS, Nat. Chem. Biol. 8 (2012) 855–861.
[19] X. Wang, D.M. Lord, S.H. Hong, W. Peti, M.J. Benedik, R. Page, T.K. Wood, Type II toxin/antitoxin MqsR/MqsA controls type V toxin/antitoxin GhoT/GhoS, Environ. Microbiol. 15 (2013) 1734–1744.
[20] B.W. Kwan, D.M. Lord, W. Peti, R. Page, M.J. Benedik, T.K. Wood, The MqsR/MqsA toxin/antitoxin system protects *Escherichia coli* during bile acid stress, Environ. Microbiol. 17 (2015) 3168–3181.
[21] B. Mui, L. Chow, M.J. Hope, Extrusion technique to generate liposomes of defined size, Methods Enzymol. 367 (2003) 3–14.
[22] T. Steinbrecher, S. Prock, J. Reichert, P. Wadhwani, B. Zimpfer, J. Burck, M. Berditsch, M. Elstner, A.S. Ulrich, Peptide-lipid interactions of the stress-response peptide TisB that induces bacterial persistence, Biophys. J. 103 (2012) 1460–1469.
[23] A.J. Krauson, J. He, W.C. Wimley, Determining the mechanism of membrane permeabilizing peptides: identification of potent, equilibrium pore-formers, Biochim. Biophys. Acta Biomembr. 1818 (2012) 1625–1632.
[24] W.C. Wimley, Describing the mechanism of antimicrobial peptide action with the interfacial activity model, ACS Chem. Biol. 5 (2010) 905–917.
[25] M. Kitagawa, T. Ara, M. Arifuzzaman, T. Ioka-Nakamichi, E. Inamoto, H. Toyonaga, H. Mori, Complete set of ORF clones of *Escherichia coli* ASKA library (a complete set of E. coli K-12 ORF archive): unique resources for biological research, DNA Res. 12 (2005) 291–299.
[26] J. Sambrook, E.F. Fritsch, T. Maniatis, Molecular Cloning: A Laboratory Manual, Cold Spring Harbor Laboratory Press, 1989.
[27] Y. Zhang, I-TASSER server for protein 3D structure prediction, BMC Bioinf. 9 (2008) 40.
[28] A. Roy, A. Kucukural, Y. Zhang, I-TASSER: a unified platform for automated protein structure and function prediction, Nat. Protoc. 5 (2010) 725–738.
[29] S.J. Marrink, H.J. Risselada, S. Yefimov, D.P. Tieleman, A.H. de Vries, The MARTINI force field: coarse grained model for biomolecular simulations, J. Phys. Chem. B 111 (2007) 7812–7824.
[30] L. Monticelli, S.K. Kandasamy, X. Periole, R.G. Larson, D.P. Tieleman, S.-J. Marrink, The MARTINI coarse-grained force field: extension to proteins, J. Chem. Theor. Comput. 4 (2008) 819–834.
[31] D.H. de Jong, G. Singh, W.D. Bennett, C. Arnarez, T.A. Wassenaar, L.V. Schafer, X. Periole, D.P. Tieleman, S.J. Marrink, Improved parameters for the martini coarse-grained protein force field, J. Chem. Theor. Comput. 9 (2012) 687–697.
[32] S.J. Marrink, A.H. de Vries, A.E. Mark, Coarse grained Model for semi-quantitative lipid simulations, J. Phys. Chem. B 108 (2004) 750–760.
[33] B. Hess, C. Kutzner, D. Van Der Spoel, E. Lindahl, GROMACS 4: algorithms for highly efficient, load-balanced, and scalable molecular simulation, J. Chem. Theor. Comput. 4 (2008) 435–447.
[34] W. Humphrey, A. Dalke, K. Schulten, VMD: visual molecular dynamics, J. Mol. Graph. 14 (1996) 33–38.
[35] C.R. Raetz, Enzymology, genetics, and regulation of membrane phospholipid synthesis in *Escherichia coli*, Microbiol. Rev. 42 (1978) 614–659.
[36] R.F. Chen, J.R. Knutson, Mechanism of fluorescence concentration quenching of carboxyfluorescein in liposomes: energy transfer to nonfluorescent dimers, Anal. Biochem. 172 (1988) 61–77.